JACS
JOURNAL OF THE AMERICAN CHEMICAL SOCIETY
Communication
pubs.acs.org/JACS

Li_2OHCl Crystalline Electrolyte for Stable Metallic Lithium Anodes

Zachary D. Hood,[†,‡,∥] Hui Wang,[†,∥] Amaresh Samuthira Pandian,[†] Jong Kahk Keum,[†,§] and Chengdu Liang*[,†]

[†]Center for Nanophase Materials Science and [§]Chemical and Engineering Materials Division, Oak Ridge National Laboratory, Oak Ridge, Tennessee 37831, United States

[‡]School of Chemistry and Biochemistry, Georgia Institute of Technology, Atlanta, Georgia 30332, United States

Supporting Information

ABSTRACT: In a classic example of stability from instability, we show that Li_2OHCl solid electrolyte forms a stable solid electrolyte interphase (SEI) layer with a metallic lithium anode. The Li_2OHCl solid electrolyte can be readily achieved through simple mixing of LiOH and LiCl precursors at a mild processing temperature <400 °C. Additionally, we show that continuous, dense Li_2OHCl membranes can be fabricated at temperatures <400 °C, standing in great contrast to current processing temperatures of >1600 °C for most oxide-based solid electrolytes. The ionic conductivity and Arrhenius activation energy were explored for the LiOH−LiCl system of crystalline solid electrolytes, where Li_2OHCl with increased crystal defects was found to have the highest ionic conductivity and reasonable Arrhenius activation energy. The Li_2OHCl solid electrolyte displays stability against metallic lithium, even in extreme conditions past the melting point of lithium metal. To understand this excellent stability, we show that SEI formation is critical in stabilizing the interface between metallic lithium and the Li_2OHCl solid electrolyte.

Advances in lithium-ion batteries within the past decade have allowed for spectacular improvements for portable computing, telecommunications, and other devices necessary for our information-rich society. These advances have also pushed our understanding of battery technology and, more specifically, the interaction between the different components within a typical battery cell. These interactions include the formation of the solid electrolyte interphase (SEI) layer between the lithium anode and the electrolyte.[1−3] Recently, there had been an increased interest in solid electrolytes, since solid electrolytes impede the formation of dendrites at the SEI and, consequently, allow for the fabrication of safer and longer-lasting batteries that can function at higher voltages.[3−6] Although various solid electrolytes show great stability with lithium anodes at higher working voltages,[7−9] current solid electrolytes have a number of key limitations: (1) it is difficult to synthesize and process large membranes consisting of oxides and phosphates; (2) sulfide-based solid electrolytes are air-sensitive; and (3) most oxide-based solid electrolytes are not compatible with metallic lithium anode.

The ideal anode for solid-state Li-ion batteries is metallic lithium because of its increased energy density.[10] Thus, efforts have moved to the development of solid electrolytes that show stability against metallic lithium to attain increased energy density.[7,8,11] Some sulfide-based solid electrolytes, such as $Li_{10}GeP_2S_{12}$, do not show stability against metallic lithium metal, which compromises the total specific energy density of the battery.[12] $Li_7La_3Zr_2O_{12}$ (LLZO) represents the only oxide-based solid electrolyte that shows stability with metallic lithium anode; however, this electrolyte displays very high interfacial resistance and requires high processing temperatures, making its implementation into solid-state batteries difficult.[13]

LiOH−LiCl electrolytes were previously explored for their increased lithium ion conductivity (10^{-4}−10^{-3} S cm^{-1} at 200 °C) and high thermodynamic decomposition voltages.[14−17] However, it was reported that LiOH−LiCl crystalline electrolytes are not stable with metallic lithium, where an apparent interfacial reaction occurs between the metallic lithium and electrolyte;[15] this interfacial reaction was not explored further. For batteries that have increased energy density, metallic lithium anode allows for a much higher capacity; however, to achieve increased energy density, the components within the cell must work in harmony, with decreased interfacial resistance and stable SEI formation. *Is it possible to have stability between a Li_2OHCl crystalline electrolyte and a molten lithium anode?* Herein, we revisit the LiOH−LiCl system to overcome the limitations of solid electrolytes. We report the mild temperature processability, ionic conductivity, Arrhenius activation energy, and metallic lithium anode compatibility of LiOH−LiCl solid electrolytes, even in extreme temperatures. In a classic example of stability from instability, we show that that Li_2OHCl forms a stable SEI with a metallic lithium anode and has the remarkable ability to cycle hundreds of times.

Straightforward Preparation of LiOH−LiCl Melt Yields Two Distinct Structures of LiOH−LiCl Crystalline Electrolytes. LiOH−LiCl solid electrolytes were prepared in a nickel crucible using methodology similar to that in previous literature.[14,17,18] Since LiOH, LiCl, and the LiOH−LiCl solid electrolytes are hygroscopic, all processes were completed under argon. LiOH (Sigma-Aldrich, ≥99%) and LiCl (Sigma-Aldrich, ≥99%) were used to create melts with the following ratios of LiOH to LiCl: 1:2, 2:3, 1:1, 3:2, and 2:1; these are referred to as Li_3OHCl_2, $Li_5(OH)_2Cl_3$, Li_2OHCl, $Li_5(OH)_3Cl_2$, and $Li_3(OH)_2Cl$, respectively. When using the same molar ratio, two distinct phases of the material may be achieved by changing the cooling treatment (Figure S1). The controlled cooling from

Received: November 12, 2015
Published: January 22, 2016

DOI: 10.1021/jacs.5b11851
J. Am. Chem. Soc. 2016, 138, 1768−1771

350 to 250 °C at 8 °C/h yields an anti-perovskite structure (termed "slow-cooled"), while fast cooling from ≥350 °C to room temperature in ∼20 min (termed "fast-cooled") gives a more complex crystal structure with increased defects due to the overcooling effect. All compounds were found to undergo a phase transition between 30 and 50 °C. This phase transition was found to significantly increase the ionic conductivity in all compounds.[19] Fast-cooled Li_2OHCl serves as a model example for this system, where the phase transition occurs reversibly, which is characterized by *in situ* powder X-ray diffraction (XRD), as shown in Figure 1. Several peaks in the XRD pattern for

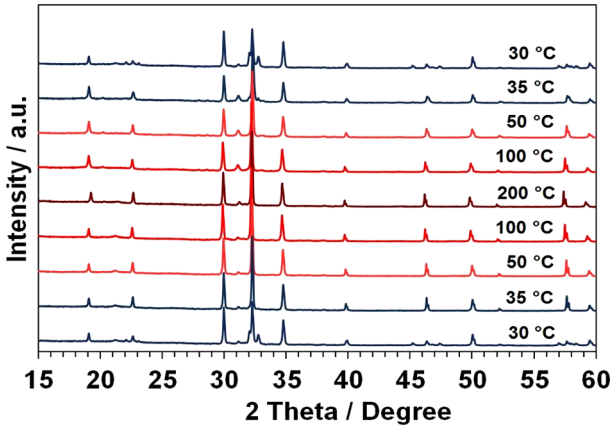

Figure 1. XRD patterns for the as-prepared, fast-cooled Li_2OHCl crystalline electrolyte from 30 to 200 °C, showing a clear phase transition from 30 to 50 °C. The blue lines correspond to the low-temperature Li_2OHCl phase, whereas the red lines correspond to the high-temperature Li_2OHCl phase. XRD confirms this phase transition is reversible.

Li_2OHCl are characteristic of this phase transition. Peaks at 22.0°, 23.0°, 32.0°, and 32.7° 2θ disappear when the electrolyte is heated from 30 to 50 °C, while the peaks at 22.5°, 32.3°, 46.4°, 57.6°, and 57.7° 2θ become more pronounced during this heating process. As shown, fast-cooled Li_2OHCl undergoes a phase change from orthorhombic to cubic at 35 °C.[17] Upon cooling the solid electrolyte from 50 to 30 °C, the peaks return to the same position as in the parent electrolyte, supporting that this phase transition is, in fact, reversible.

Li_2OHCl from Fast Cooling Shows Enhanced Ionic Conductivity and Lower Activation Energy at Increased Temperatures. The ionic conductivity and Arrhenius activation energy were measured for each LiOH−LiCl compound. The crystalline electrolytes were cold-pressed in a specialized pressurized cell with Al/C blocking electrodes at 300 MPa, and electrochemical impedance spectroscopy (EIS) measurements were collected between 1 MHz and 1 Hz with amplitude of 100 mV. When cold-pressed, LiOH−LiCl electrolytes form dense pellets free of fractures. Because LiOH−LiCl crystalline electrolytes exhibit a phase transition between 30 and 50 °C, the Arrhenius activation energy was calculated for temperatures ≥50 °C. Representative EIS measurements are shown for fast-cooled Li_2OHCl in Figure S2.

When comparing the resulting crystalline electrolytes from the fast cooling and slow cooling procedures, the ionic conductivities of the electrolytes at 25 °C share a similar trend. At 25 °C, fast-cooled $Li_5(OH)_2Cl_3$ yields the best ionic conductivity of 1.48×10^{-7} S cm^{-1} (Figure 2). When heated to 100 °C, the electrolytes from the fast cooling method maintain ionic conductivities nearly

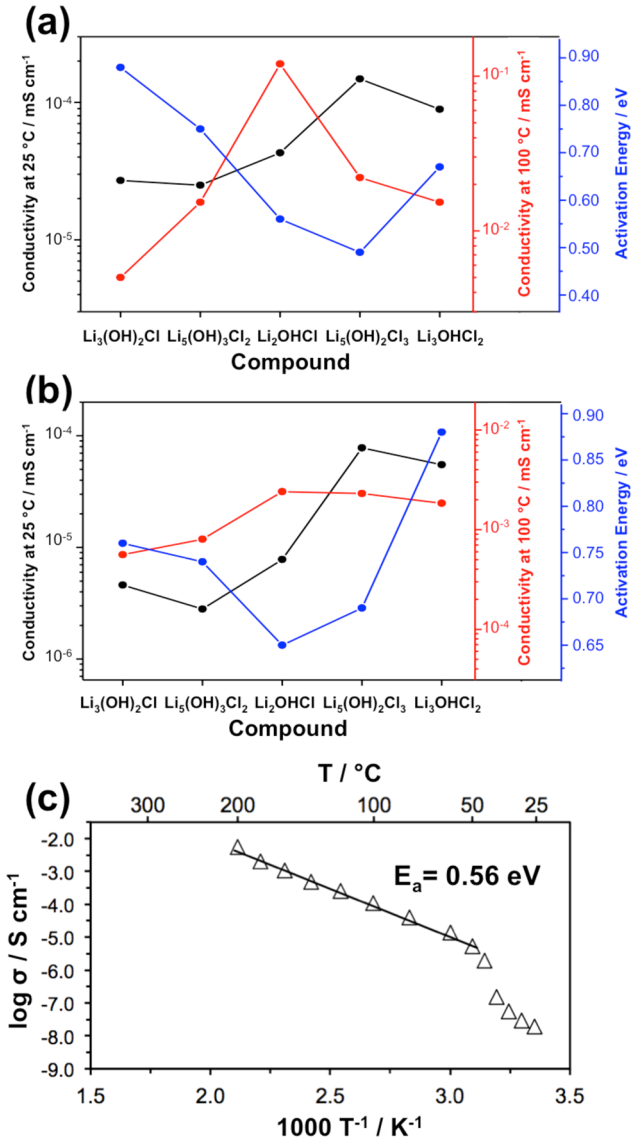

Figure 2. Ionic conductivity at 25 °C (black line) and 100 °C (red line), and Arrhenius activation energy after the phase transition (blue line) for LiOH−LiCl crystalline electrolytes from (a) the fast cooling procedure and (b) the slow cooling procedure. (c) Arrhenius plot for fast-cooled Li_2OHCl, which exhibits the highest ionic conductivity at 100 °C and maintains a reasonable Arrhenius activation energy of 0.56 eV.

1 order of magnitude higher than those from the slow cooling procedure. This enhancement in ionic conductivity from fast cooling is attributed to an increase of defects in the crystal lattice. Defects have previously been shown to enhance the ionic conductivity in crystalline electrolytes by creating an increased concentration of vacancies and interstitial spaces, and for the case of LiOH−LiCl crystalline electrolytes, creating defects through the utilization of the overcooling effect significantly improves the ionic conductivity at increased temperatures.[14,15,17]

An equivalent stoichiometric ratio of LiOH and LiCl allows the ionic conductivity to reach a maximum at 100 °C for electrolytes from both the slow cooling and fast cooling methods. An excess of either hydroxide or chloride character yields an unfavorable charge carrier distribution after the crystalline electrolytes undergo the phase transition at increased temperatures.[20,21] Additionally, the Arrhenius activation energy reaches a minimum (<0.60 eV) for Li_2OHCl and $Li_5(OH)_2Cl_3$ from the

DOI: 10.1021/jacs.5b11851
J. Am. Chem. Soc. 2016, 138, 1768−1771

fast cooling method, making these electrolytes more favorable for solid-state battery applications. Fast-cooled Li_2OHCl has the highest ionic conductivity at increased temperatures and Arrhenius activation energy of 0.56 eV, rendering this electrolyte of interest for further exploration.

Melt-Casting Li_2OHCl Yields Continuous, Dense Membranes. A critical limitation of most oxide-based solid electrolytes lies in the fact that it is hard to process continuous, dense membranes at decreased temperatures. In fact, most oxide-based solid electrolytes require processing temperatures >1600 °C to form dense membranes for solid-state battery applications. Li_2OHCl can be processed into continuous, dense membranes at much milder temperatures <400 °C. To fabricate these membranes, the molten Li_2OHCl mixture was poured into a Teflon cast (Figure S3), and the melt was pressed slightly with a Teflon plunger (<1 MPa); the resulting membranes were dense and free of pores and cracks (Figure 3). When no pressure is applied to Li_2OHCl upon cooling in the Teflon mold, cracks and voids appear in the solid electrolyte membrane (Figure S4), which justifies the use of a Teflon plunger. Melt-casting at a mild temperature demonstrates that Li_2OHCl is a promising candidate for large-scale production of continuous, dense electrolyte membranes.

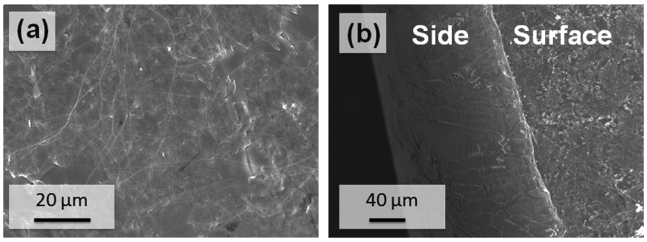

Figure 3. SEM images of (a) the surface and (b) a side view (tilt angle: 45°) of the pressed Teflon-cast Li_2OHCl electrolyte, which yields continuous, dense membranes.

Li_2OHCl Shows Superior Performance against Molten Lithium Anode. To demonstrate the performance and long-term compatibility of fast-cooled Li_2OHCl against molten lithium anode, Li/Li_2OHCl/Li symmetric cells were fabricated.[22] These cells were assembled by pressing a 1/2 in. pellet of highly ionic-conducting ball-milled Li_2OHCl at 300 MPa inside a specialized cell developed by our group.[9] For the purpose of assessing the compatibility of Li_2OHCl with molten lithium anode, cold pressing allows the solid electrolyte to form a continuous network with the body of the specialized cell. Additionally, at high pressures, Li_2OHCl maintains good compactness (>90% of the theoretical density). Then, metallic lithium foil (≤15 mg, 12 mm in diameter and thickness of ∼100 μm) was deposited with carbon mesh on each side of the pellet. A spring fixated within the cell ensured good contact between the lithium and solid electrolyte. Li_2OHCl solid electrolyte shows stability with metallic lithium, even at temperatures above the melting point of lithium metal. Upon heating the cells to 195 °C, the electrolyte shows great cyclability with molten lithium anode. Figure 4 demonstrates favorable lithium exchange for 4500 min with an ideal cell voltage retention of 0.06 V (cycling data for 14 000 min and at different current densities are provided in Figures S5 and S6). Typically, solid electrolytes require relatively smaller current densities (0.01−0.2 mA) when cycled with metallic lithium, but for the molten phase, the Li anode allows for a larger current density (1.0 mA), which allows for faster charging kinetics.

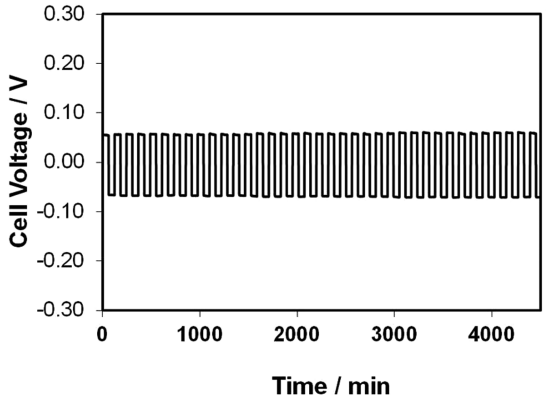

Figure 4. Molten lithium cyclability in a symmetric Li/Li_2OHCl/Li cell with a current density of 1.0 mA cm^{-2} at 195 °C, demonstrating stability between the molten lithium anode and the crystalline electrolyte.

This cycling performance is attributed to the formation of a stable SEI. The direct-current (dc) conductivity from polarization is 1.5×10^{-3} S cm^{-1}, which holds a good correlation with the alternating-current (ac) conductivity of 2.8×10^{-3} S cm^{-1}, for fast-cooled Li_2OHCl at 195 °C. The differences in the dc and ac cell conductivity results relate to SEI formation and the different electrodes utilized for each measurement. Negligible interfacial resistance was observed when the Li_2OHCl crystalline electrolyte was cycled with molten lithium anode for >400 cycles, even after SEI formation.

To further demonstrate the stability of Li_2OHCl with molten lithium anode after SEI formation, SEM images with energy-dispersive X-ray spectroscopy (EDX) of symmetric cells were collected; this method was previously shown as a powerful tool to visualize interfaces in batteries.[6,23−26] A cross section of the Li/Li_2OHCl/Li symmetric cell cycled at 195 °C for 160 cycles shows a clear SEI formation (Figure 5). The SEI has a higher concentration of oxygen determined by EDX, and the thickness of this layer is 50 μm across the interface, which supports the interfacial reaction between molten lithium and Li_2OHCl to form Li_2O, LiCl, and the gaseous byproduct H_2 shown below:

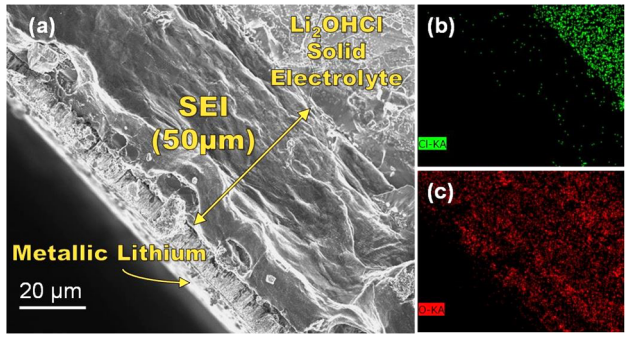

Figure 5. SEM image of Li/Li_2OHCl/Li symmetric cell after 160 charge/discharge cycles showing (a) the cross section of the SEI with correlating EDX mapping of (b) chlorine in green and (c) oxygen in red. The SEI layer is uniform and measures 50 μm in thickness.

$$2Li_2OHCl_{(s)} + 2Li_{(l)} \rightarrow 2Li_2O_{(s)} + 2LiCl_{(s)} + H_{2(g)}$$

LiCl remains closer to the Li_2OHCl solid electrolyte, while Li_2O is in higher concentration closer to the lithium anode and

DOI: 10.1021/jacs.5b11851
J. Am. Chem. Soc. 2016, 138, 1768−1771

constitutes the bulk of the SEI, forming an interconnected network that protects the crystalline Li_2OHCl from further reactions with molten lithium anode. H_2 is suspected to evolve from the interface and does not contribute to the formation of pores or cracks in the SEI nor solid electrolyte. SEM images with EDX mapping of the surface layers in $Li/Li_2OHCl/Li$ symmetric cells support SEI formation primarily constituting Li_2O (Figure S7). This SEI is believed to contain unreacted lithium metal, as the interfacial reaction between the molten lithium and Li_2OHCl is self-limiting. Simultaneously, the SEI allows the molten lithium anode to cycle hundreds of times with crystalline Li_2OHCl solid electrolyte. Still, this result raises the question: *To what extent does this SEI form?*

The formation kinetics of the SEI layer were determined by constructing similar symmetric cells with the same amount of lithium anode, charged/discharged for 40 cycles, and subsequently disassembled to measure the thickness of the SEI. After 40 cycles, the cells have the same SEI thickness as the cells cycled 160 times (Figure S8). The SEI layer is dense and free from pores and cracks after both 40 and 160 cycles, supporting the fact that the interfacial reaction between the Li_2OHCl solid electrolyte and the molten lithium anode occurs rapidly, which matches the criteria for an ideal SEI.[27] Since the thickness of the SEI layer does not significantly increase from cycle 40 to 160 for the symmetric cells, the interfacial reaction is believed to be self-limiting, which allows for symmetric cells of $Li/Li_2OHCl/Li$ to cycle repeatedly and maintain a lower interfacial resistance.

To summarize, we explored the LiOH−LiCl system to overcome the limitations of solid electrolytes. We found that fast-cooled Li_2OHCl has a number of excellent properties for solid-state batteries plus an extremely stable interface with metallic lithium anode through self-limiting interfacial reactions. Cold-pressed Li_2OHCl from fast cooling exhibited the highest ionic conductivity and practical Arrhenius activation energy at increased temperatures. Li_2OHCl shows compatibility with metallic lithium, even in extreme temperatures. $Li/Li_2OHCl/Li$ cells cycled at 195 °C show stability between the solid electrolyte and molten lithium anode upon SEI formation, where the electrolyte and lithium show little interfacial resistance and can cycle hundreds of times. The SEI was found to have a higher concentration of oxygen, supporting the formation of a lithium oxide layer, which stabilizes the molten lithium anode with the solid electrolyte without adversely compromising the ionic conductivity. This finding opens ample opportunities for advancements in batteries that employ metallic lithium anode.

■ ASSOCIATED CONTENT

Supporting Information

The Supporting Information is available free of charge on the ACS Publications website at DOI: 10.1021/jacs.5b11851.

Experimental methods, materials characterization using XRD, SEM, and EDX, and related discussion, including Figures S1−S8 (PDF)

■ AUTHOR INFORMATION

Corresponding Author

*cd_liang@hotmail.com

Author Contributions

‖Z.D.H. and H.W. contributed equally to this publication.

Notes

The authors declare no competing financial interest.

■ ACKNOWLEDGMENTS

This work was sponsored by the U.S. Department of Energy (DOE), Office of Science, Basic Energy Sciences, Materials Sciences and Engineering Division. The synthesis and characterization was completed at the Center for Nanophase Materials Science, which is a DOE Office of Science User Facility. Z.D.H. was supported by Higher Education Research Experiences (HERE) at Oak Ridge National Laboratory. Also, Z.D.H. gratefully acknowledges support from the National Science Foundation Graduate Research Fellowship under Grant No. DGE-1148903 and the Georgia Tech-ORNL Fellowship.

■ REFERENCES

(1) Peled, E. *J. Electrochem. Soc.* **1979**, *126*, 2047.
(2) Peled, E. *J. Power Sources* **1983**, *9*, 253.
(3) Winter, M. *Z. Phys. Chem.* **2009**, *223*, 1395.
(4) Li, J.; Baggetto, L.; Martha, S. K.; Veith, G. M.; Nanda, J.; Liang, C.; Dudney, N. J. *Adv. Energy Mater.* **2013**, *3*, 1275.
(5) Li, J.; Dudney, N. J.; Nanda, J.; Liang, C. *ACS Appl. Mater. Interfaces* **2014**, *6*, 10083.
(6) Unemoto, A.; Ikeshoji, T.; Yasaku, S.; Matsuo, M.; Stavila, V.; Udovic, T. J.; Orimo, S.-I. *Chem. Mater.* **2015**, *119*, 13459.
(7) Rangasamy, E.; Liu, Z.; Gobet, M.; Pilar, K.; Sahu, G.; Zhou, W.; Wu, H.; Greenbaum, S.; Liang, C. *J. Am. Chem. Soc.* **2015**, *137*, 1384.
(8) Liu, Z.; Fu, W.; Payzant, E. A.; Yu, X.; Wu, Z.; Dudney, N. J.; Kiggans, J.; Hong, K.; Rondinone, A. J.; Liang, C. *J. Am. Chem. Soc.* **2013**, *135*, 975.
(9) Wang, H.; Ma, C.; Chi, M.; Liang, C. *Adv. Mater. Interfaces* **2015**, DOI: 10.1002/admi.201500268.
(10) Zu, C.-X.; Li, H. *Energy Environ. Sci.* **2011**, *4*, 2614.
(11) Li, J.; Ma, C.; Chi, M.; Liang, C.; Dudney, N. J. *Adv. Energy Mater.* **2015**, *5*, 1401408.
(12) Kamaya, N.; Homma, K.; Yamakawa, Y.; Hirayama, M.; Kanno, R.; Yonemura, M.; Kamiyama, T.; Kato, Y.; Hama, S.; Kawamoto, K. *Nat. Mater.* **2011**, *10*, 682.
(13) Wolfenstine, J.; Allen, J.; Read, J.; Sakamoto, J. *J. Mater. Sci.* **2013**, *48*, 5846.
(14) Hartwig, P.; Rabenau, A.; Weppner, W. *J. Less-Common Met.* **1981**, *78*, 227.
(15) Hartwig, P.; Weppner, W. *Solid State Ionics* **1981**, *3*, 249.
(16) Zhao, Y.; Daemen, L. L. *J. Am. Chem. Soc.* **2012**, *134*, 15042.
(17) Schwering, G.; Hönnerscheid, A.; van Wüllen, L.; Jansen, M. *ChemPhysChem* **2003**, *4*, 343.
(18) Friese, K.; Hönnerscheid, A.; Jansen, M. *Z. Kristallogr. - Cryst. Mater.* **2003**, *218*, 536.
(19) Eilbracht, C.; Kockelmann, W.; Hohlwein, D.; Jacobs, H. *Phys. B* **1997**, *234*, 48.
(20) Maier, J.; Münch, W. *Z. Anorg. Allg. Chem.* **2000**, *626*, 264.
(21) Braga, M. H.; Stockhausen, V.; Oliveira, J. C.; Ferreira, J. A. *MRS Online Proc. Libr.* **2013**, *1526*, mrsf12.
(22) Burns, J.; Krause, L.; Le, D.-B.; Jensen, L.; Smith, A.; Xiong, D.; Dahn, J. *J. Electrochem. Soc.* **2011**, *158*, A1417.
(23) Unemoto, A.; Chen, C.; Wang, Z.; Matsuo, M.; Ikeshoji, T.; Orimo, S.-i. *Nanotechnology* **2015**, *26*, 254001.
(24) Kotobuki, M.; Suzuki, Y.; Munakata, H.; Kanamura, K.; Sato, Y.; Yamamoto, K.; Yoshida, T. *Electrochim. Acta* **2011**, *56*, 1023.
(25) Ota, H.; Sato, T.; Suzuki, H.; Usami, T. *J. Power Sources* **2001**, *97*, 107.
(26) Lu, P.; Li, C.; Schneider, E. W.; Harris, S. J. *J. Phys. Chem. C* **2014**, *118*, 896.
(27) Verma, P.; Maire, P.; Novák, P. *Electrochim. Acta* **2010**, *55*, 6332.

■ NOTE ADDED AFTER ASAP PUBLICATION

The uncorrected version of this paper posted ASAP on January 27, 2016; the corrected version reposted on February 2, 2016.

DOI: 10.1021/jacs.5b11851
J. Am. Chem. Soc. 2016, 138, 1768−1771